BIOMOLECULES & THERAPEUTICS

Original Article
Biomol Ther 33(3), 447-457 (2025)

Microplastics Accumulation Induces Kynurenine-Derived Neurotoxicity in Cerebral Organoids and Mouse Brain

Sung Bum Park[1,†], Jeong Hyeon Jo[1,2,†], Seong Soon Kim[1,†], Won Hoon Jung[1], Myung-Ae Bae[1], Byumseok Koh[1,3,*] and Ki Young Kim[1,*]

[1]*Therapeutics and Biotechnology Division, Korea Research Institute of Chemical Technology (KRICT), Daejeon 34114,*
[2]*Graduate School of New Drug Discovery and Development, Chungnam National University, Daejeon 34134,*
[3]*Medicinal Chemistry & Pharmacology, University of Science & Technology (UST), Daejeon 34113, Republic of Korea*

Abstract

Microplastics (MP) are pervasive environmental pollutants with potential adverse effects on human health, particularly concerning neurotoxicity. This study investigates the accumulation and neurotoxic effects of MP in cerebral organoids and mouse brains. Utilizing *in vitro* cerebral organoids and *in vivo* mouse models, we examined the penetration of MP, revealing that smaller MP (50 nm) infiltrated deeper into the organoids compared to larger ones (100 nm). Exposure to 50 nm MP resulted in a significant reduction in organoid viability. Furthermore, total RNA sequencing indicated substantial alterations in neurotoxicity-related gene expression. *In vivo*, MP-treated mice exhibited notable DNA fragmentation in the hippocampus and cortex, alongside elevated levels of inflammatory markers and neurotoxic metabolites, such as kynurenine (KYN) and 3-hydroxykynurenine (3-HK). Our findings suggest that MP may promote neurotoxicity through the kynurenine pathway, leading to heightened levels of neurotoxic compounds like quinolinic acid. This research highlights the potential for MP to induce neuroinflammatory responses and disrupt normal brain function, underscoring the need for further investigation into the long-term effects of MP exposure on neurological health.

Key Words: Microplastics, Cerebral organoids, *In vivo* study, Kynurenine-derived neurotoxicity, Apoptosis, Inflammation

INTRODUCTION

Microplastics (MP), small plastic particles less than 5 millimeters in size, have become a pervasive environmental pollutant with far-reaching consequences for both human health and the environment (Vethaak and Legler, 2021). These particles originate from various sources, including the breakdown of larger plastic debris, the shedding of microfibers from textiles, and the release of microbeads from personal care products (Hale *et al*., 2020). Regarding human health, concerns have been raised about the ingestion of MP due to their potential to accumulate in the body (Mohamed Nor *et al*., 2021). Studies suggest that MP can penetrate the gastrointestinal tract, and their small size enables them to be transported to various organs and tissues, potentially leading to systemic effects (Cocci *et al*., 2022). Furthermore, MP can absorb and accumulate toxic chemicals from the surrounding environment, such as persistent organic pollutants and heavy metals (Fu *et al*., 2021; Lu *et al*., 2023). When ingested, these chemicals may be released, causing adverse health effects, including endocrine disruption, immune system impairment, and even carcinogenicity (Xu *et al*., 2022; Yuan *et al*., 2022).

The impact of MP on human health is a growing concern; however, there is limited understanding of their potential accumulation in the brain (Pitt *et al*., 2018). Recent studies suggest that MP can translocate from the gastrointestinal tract to various organs and tissues, including the liver, kidneys, and lungs (Rivers-Auty *et al*., 2023). Emerging evidence also indicates that certain nanoparticles and small particles can traverse the blood-brain barrier (BBB) under specific conditions (Zhou *et al*., 2018). Furthermore, research suggests that MP can cross the BBB, leading to neurotoxicity, neuroinflammation, and brain injury by disrupting the secretion of neuroinflammatory chemokines, cytokines, transporters, and receptor mark-

Open Access **https://doi.org/10.4062/biomolther.2024.185**

Received Oct 10, 2024 **Revised** Dec 10, 2024 **Accepted** Dec 14, 2024
Published Online Apr 4, 2025

***Corresponding Authors**
E-mail: bkoh@krict.re.kr (Koh B), kykim@krict.re.kr (Kim KY)
Tel: +82-42-860-74645 (Koh B), +82-42-860-7471 (Kim KY)
Fax: +82-42-861-0770 (Koh B), +82-42-861-0770 (Kim KY)
[†]The first three authors contributed equally to this work.

ers (Kaushik *et al*., 2024). It is plausible that MP, particularly smaller ones, could breach the BBB and enter the brain (Jin *et al*., 2022; Lee *et al*., 2022). Once in the brain, MP may interact with neural tissue and cause adverse effects, such as inflammation, oxidative stress, and disruption of normal neuronal signaling processes (Jeong *et al*., 2022; Teng *et al*., 2022). Additionally, MP can adsorb and carry toxic chemicals that, when released in the brain, exacerbate their harmful effects.

Cerebral organoids, three-dimensional *in vitro* models that mimic the structural and functional complexity of the human brain (Parmentier *et al*., 2023), have emerged as a promising tool for studying the effects of environmental toxic substances. The use of cerebral organoids offers several advantages for evaluating MP toxicity (Fan *et al*., 2022; Li *et al*., 2022). They provide a more physiologically relevant platform compared to traditional cell culture systems and allow for long-term monitoring of cellular responses (Lancaster *et al*., 2013; Pollen *et al*., 2019; Kelley and Pașca, 2022). Additionally, cerebral organoids offer the opportunity to study the specific effects of different types of MP, such as particles of varying sizes or chemical compositions. To assess the impact of MP on brain tissue, cerebral organoids can be exposed to controlled concentrations of MP particles (Hua *et al*., 2022). This approach allows for the investigation of MP' potential effects on neuronal development, synaptic connectivity, and overall brain functionality (Cakir *et al*., 2019; Qian *et al*., 2019; Velasco *et al*., 2019). Moreover, by utilizing advanced imaging techniques and molecular analyses, researchers can monitor cellular responses and alterations in gene expression within the organoids (Brémond Martin *et al*., 2021).

Early research on MP accumulation in the brain suggests that these particles may have a negative impact on neurological health. However, further research is needed to determine the extent of MP accumulation in the brain, its long-term effects, and how MP interact with neural tissue. This understanding is crucial for developing effective strategies to reduce the risks of MP exposure and protect brain health. In this study, we used *in vitro* cerebral organoids and *in vivo* mouse models to systematically investigate the neurotoxicity of MP.

MATERIALS AND METHODS

Human cerebral organoid culture

Cerebral organoids were cultured and differentiated for over 120 days according to a previous protocol (Xiang *et al*., 2017) with slight modifications. Briefly, 2×10^4 induced pluripotent stem cells (iPSCs; IMR90-4, WiCell, Madison, WI, USA) were seeded into each well of a U-bottom ultralow-attachment 96-well plate (Corning, Corning, NY, USA) in the presence of neural induction media (NIM) [Dulbecco's modified Eagle medium/nutrient mixture F-12 (Invitrogen, Carlsbad, CA, USA) containing 1% Glutamax (Invitrogen), 1% MEM-NEAA (Invitrogen), 15% knockout serum (Invitrogen), 0.1 nM β-mercaptoethanol (Sigma-Aldrich, St. Louis, MO, USA), 100 nM LDN-193189 (Sigma-Aldrich), 10 μM SB431542 (Sigma-Aldrich), and 2 μM XAV939 (Sigma-Aldrich)] and cultured for 10 days. The media were changed every other day. After 10 days of static culture, cerebral organoids were transferred into ultralow-attachment 6-well plates (Corning) in the presence of neural differentiation media (NDM-I) [DMEM/F12 mixed with an equal volume of neurobasal media (Corning) containing N2 supplement (Invitrogen), B27 supplement without vitamin A (Invitrogen), 1% MEM-NEAA, 1% Glutamax, and human insulin solution (Sigma-Aldrich)] and cultured for 8 days with orbital shaking at 80 rpm. For neural maturation, cerebral organoids were cultured in neural differentiation media (NDM-II) containing B27 supplemented with vitamin A (Invitrogen), brain-derived neurotrophic factor (BDNF, Sigma-Aldrich), cyclic adenosine monophosphate (cAMP, Sigma-Aldrich), and ascorbic acid (Sigma-Aldrich), which were replaced every 4 days from day 18.

MP preparation and treatment

Fifty- (50 MP) and 100-micron (100 MP) microplastic beads conjugated with fluorescent dyes (Fluoresbrite® dyed particles, MP) were purchased from Polysciences (Warrington, PA, USA). Both 50 μm and 100 μm MP were autoclaved (121°C and 0.12 Mpa) prior to experiments. For evaluating the impact of MP, cerebral organoids cultured for 120 days were used. The delivery medium for MP in cerebral organoids was NDM-II. Both 50 μm and 100 μm MP were treated in cerebral organoids at a concentration of 10 mg/mL for 3 weeks (21 days). In animal experiments, saline was used as the delivery medium. MP at a concentration of 2.5 mg/mL were administered orally every day for 7 days at a dose of 200 μL. All MP stock solutions used in this study were sterilized before use.

Organoid and tissue histology

Cerebral organoids were fixed with 4% paraformaldehyde (Sigma-Aldrich) for 30 min at 4°C. For vibratome sectioning, the fixed organoids were embedded in 3% agarose gel. The mouse brain was used for vibratome sectioning without fixation, and only the left brain tissues were used (Samy *et al*., 2023). Slicing of cerebral organoid and brain tissue was performed using a 7000 SMZ vibratome (Campden Instruments, Loughborough, UK) in PBS (Sigma-Aldrich) at a speed of 0.3 mm/s, 1.00 mm amplitude, and 50 Hz. Then, 300 μm cerebral organoid slices were peeled off at a time from the sample and gathered using a small art brush. For cryostat sectioning, the organoids were incubated in a 30% sucrose solution in phosphate-buffered saline (PBS, pH 7.4, Corning) for 1 day at 4°C until they sank. Organoids were then embedded in OCT compound (Sakura Finetek, Torrance, CA, USA) and frozen at −80°C. A Cryotome (Leica, CM-1850, Wetzlar, Germany) was used for preparing sections, and tissues were sectioned at −25°C with an 8 μm thickness. After sectioning, the tissues were washed with PBS for 30 min to remove the residual OCT compound.

Total RNA sequencing

RNA sequencing was performed according to previous reports (Kang *et al*., 2022). Briefly, the total RNA concentration was measured using Quant-IT RiboGreen (Invitrogen, #R11490). RNA integrity was assessed by running samples on the TapeStation using RNA screentape (Agilent Technologies, Santa Clara, CA, USA). The RNA isolated from each sample was used to construct sequencing libraries with the SMARTer Universal Low Input RNA Kit for Sequencing, following the manufacturer's protocol. After rRNA depletion, first-strand cDNA synthesis was initiated using the SMART N6 CDS Primer, followed by template switching with the SMARTer II oligonucleotide at the 5' end of the transcript. The first-strand cDNA selectively bound to SPRI beads, allowing con-

taminants to remain in solution, which were then removed by magnetic separation. The beads were used directly for PCR amplification. The Advantage 2 Polymerase Mix was used for efficient amplification of cDNA templates via long-distance PCR. PCR-amplified cDNA was purified by immobilization on AMPure XP beads, washed with 80% ethanol, and eluted with an elution buffer. The amplified cDNA was digested with RsaI to remove the SMART adapter, followed by end repair, addition of a single 'A' base, and ligation of indexing adapters. The products were purified and enriched by PCR to create the final cDNA library. The libraries were quantified using qPCR (KAPA Library Quantification kits for Illumina Sequencing platforms) and assessed for quality with the Agilent Technologies 4200 TapeStation. Indexed libraries were sequenced using the NovaSeq platform (Illumina, San Diego, CA, USA) by Macrogen (Seoul, Korea).

RNA isolation and quantitative PCR (qPCR)

qPCR was conducted according to a previous report (Han *et al*., 2023). To isolate RNA from cerebral organoids, the RNeasy Mini Kit (Qiagen, Hilden, Germany) was used according to the manufacturer's instructions. RNA quality and quantity were assessed using a NanoDrop 2000 instrument (Thermo Fisher Scientific, Waltham, MA, USA). Next, 2 μg of RNA was reverse transcribed to cDNA using the RT2 First Strand Kit (Qiagen). The expression of 84 key neurotoxicity genes was evaluated using the Human Neurochemical, Neurotoxicity, and CD RT2 Profiler PCR Array (PAHS-169ZR; PAHS-404ZR; PAHS-060ZR; PAHS-096ZR) with SYBR Green chemistry (RT2 SYBR Green ROX qPCR Mastermix; Qiagen) on the Rotor-Gene Q instrument (Qiagen). Gene expression was normalized to the geometric mean of five housekeeping reference genes (ACTB, B2M, GAPDH, HPRT1, and RPLP0), determined using RefFinder algorithm analysis (GeneGlobe, Qiagen).

Western blot analysis

Cerebral organoids were collected and lysed in ice-cold RIPA buffer (Thermo Fisher Scientific) containing protease inhibitors (Roche, Basel, Switzerland). Protein concentrations were determined using a BCA protein assay kit (Pierce Biotechnology, Waltham, MA, USA). Equal amounts of protein were subjected to electrophoresis using 10% sodium dodecyl sulfate-polyacrylamide gels (Bio-Rad Laboratories, Hercules, CA, USA, Park *et al*., 2024). After transfer to polyvinylidene fluoride membranes (Bio-Rad Laboratories), the proteins were hybridized with primary antibodies against: BCL-2, BAX, cytochrome C, caspase-3, cleaved caspase-3, choline O-acetyltransferase (ChAT), glutamate decarboxylase 2 (GAD2), vesicular glutamate transporter 2 (VGLUT2), tyrosine hydroxylase (TH), and ß-actin (Cell Signaling Technology, CST, Danvers, MA, USA), followed by incubation with horseradish peroxidase (HRP)-conjugated secondary antibodies (Thermo Fisher Scientific). Protein bands were visualized using a Chemidoc MP System (Bio-Rad Laboratories). β-actin was used as the protein loading control.

Proteome profiler cytokine array

Cerebral organoids and mouse brains were lysed in RIPA buffer and centrifuged at 4°C and 15,000 RPM. The Proteome Profiler Human (Cat. No. ARY005B) and Mouse (Cat. No. ARY028) Cytokine Array Kits (R&D Systems, Minneapolis, MN, USA) were used according to the manufacturer's instructions. The supernatant of cerebral organoid and mouse brain samples was processed, and images were captured using the Bio-Rad Laboratories ChemiDoc MP image system. Signal analysis was performed by measuring pixel density using Bio-Rad Laboratories Image Lab ver. 6.1.0 software.

Human cerebral organoid staining & viability assay

For dead cell staining, cerebral organoids were incubated with 10 mg/mL EthD-1 (RFP, Thermo Fisher Scientific) for 30 min at 37°C, following the manufacturer's protocol. The organoids were then imaged using an Eclipse Ti2 microscope (Nikon, Japan). For the viability assay, organoids were quantitatively analyzed using the CellTiter-Glo® 3D cell viability assay kit (Promega, Madison, WI, USA). At the indicated time points following MP treatment, the luminescence generated by the reaction was measured using a microplate reader (SpectraMax iD5, Molecular Devices, San Jose, CA, USA) and presented as a dose-response curve.

Neurotransmitter analysis

Quantitative analysis of eight neurotransmitters was performed using ultra-performance liquid chromatography (ACQUITY UPLC System, Waters Corporation, Milford, MA, USA) coupled with a Xevo TQ-S triple quadrupole mass spectrometer (Waters Corporation), following a previously reported method (Kim *et al*., 2021). Cerebral organoids were washed three times with 0.1 M PBS. Equal amounts of organoids were then added to distilled water containing 1% formic acid and homogenized using a probe-type sonicator (Ultrasonic Processor VCX-130, Sonics & Materials Inc., Newtown, CT, USA). Each homogenate was centrifuged at 15,000 rpm for 20 min at 4°C. The supernatants were extracted by adding an equal volume of methanol containing 1% formic acid, vortexing, and centrifuging at 15,000 rpm for 10 min at 4°C. Clear supernatants were transferred into LC vials for analysis. The concentrations of the eight neurotransmitters were normalized to the protein content of the organoid homogenate following LC–MS/MS analysis.

Animal care & experimentation

Male C57BL/6 mice, aged eight weeks, were obtained from Orient Bio (Seongnam, Korea). The mice were housed in a specific pathogen-free animal room with controlled environmental conditions, including a temperature of 23 ± 2°C, humidity maintained at 55-60%, and a 12/12-h light/dark cycle. A minimum acclimation period of one week was provided before experimentation. The standard laboratory animal feed was supplied by Biopia (Gunpo, Korea) and was freely accessible to the mice, along with water. The experimental animals were orally administered 10 mg/mL (1 mL) daily for seven days. Their weights were measured on the first and last days of the study. All *in vivo* experimental procedures were conducted in accordance with the guidelines of the Animal Research Committee of the Korea Institute of Chemical Technology (2023-7A-07-09).

TUNEL assay

The TUNEL assay was conducted following a previously described protocol (Jeong *et al*., 2024). The DeadEnd Colorimetric TUNEL System (G7360, Promega) was used.

Statistical analysis

Data are presented as the mean ± standard error of the mean (SEM). Results were obtained from three independent experiments, with each group consisting of a minimum of four to six samples. Statistical analysis was conducted using GraphPad Prism (Boston, MA, USA), Qiagen GeneGlobe (Hilden, Germany). Statistical significance was evaluated using Student's *t*-test for independent samples or one-way ANOVA followed by Tukey's multiple comparisons test. Significance levels were set at $^{\#}p<0.05$, $^{\#\#}p<0.01$, and $^{\#\#\#}p<0.001$.

RESULTS

MP penetration into cerebral organoids

The aim of this study was to investigate the harmful effects of MP on the brain (Fig. 1A). Fully matured cerebral organoids were used to mimic *in vivo* conditions and assess the impact of MP exposure. The organoids, differentiated for 90 days, consisted of neurons and glial cells, including astrocytes and microglia (data not shown). Initially, we examined the differences in MP penetration based on particle size. Accumulation of MP was observed at various points in the 50 MP treatment group, which was more pronounced compared to the 100 MP group (Fig. 1B). Notably, 50 MP accumulated deep within the organoids, penetrating to depths greater than 300 μm and following the natural folds of the organoid structure (Fig. 1C, red arrow). We also monitored the concentration-dependent viability of the cerebral organoids (Fig. 1D). The data suggest that both 50 MP and 100 MP caused a decrease in organoid viability of more than 10% at a concentration of 1,000 ng/mL. The apoptotic response induced by MP exposure was confirmed using ethidium homodimer-1 (EthD-1) staining (Fig. 1E). A TUNEL assay further verified MP-induced

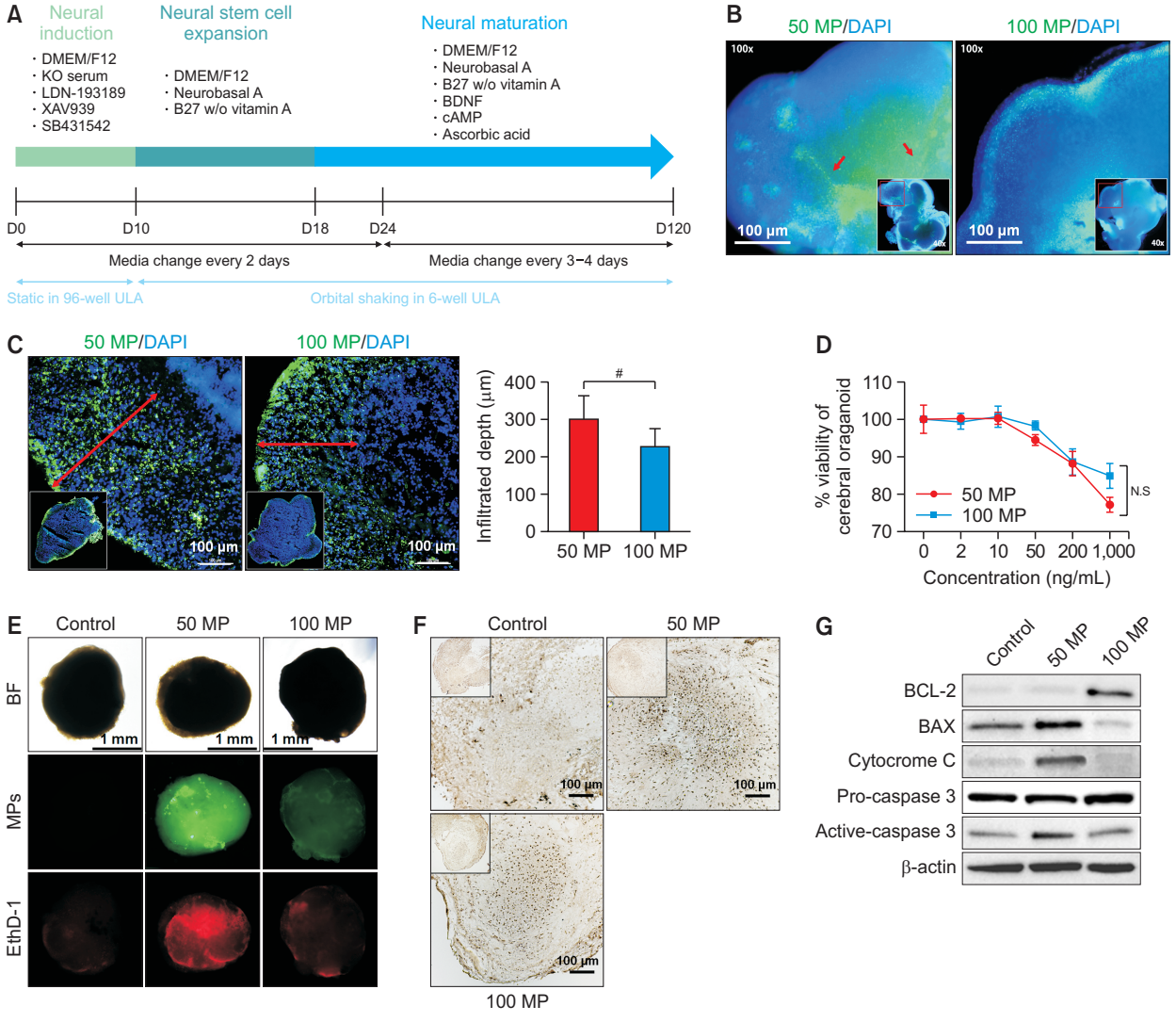

Fig. 1. MP penetration and viability changes in cerebral organoids. (A) Cerebral organoid culture and MP treatment scheme. (B, C) Fluorescence images of cerebral organoids exposed to 50 nm and 100 nm MPs. (D) Viability changes. (E, F) Dead cell quantification. (G) Apoptotic marker expression levels in cerebral organoids following MP administration. Error bars represent the standard error of the mean from six independent experiments. $^{\#}p<0.05$.

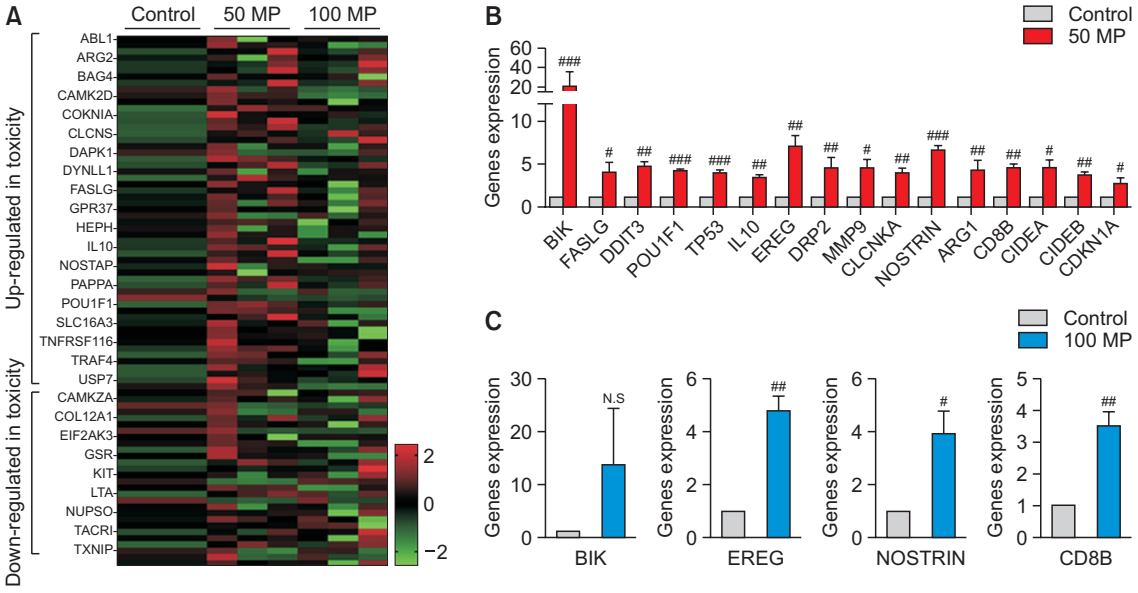

Fig. 2. Effect of MPs on neurotoxicity in cerebral organoids. (A) Heatmap of changes in neurotoxicity-related gene expression levels. (B, C) Neurotoxicity in cerebral organoids exposed to 50 nm and 100 nm MPs, respectively. Error bars represent the standard error of the mean from three independent experiments. $^{\#}p<0.05$, $^{\#\#}p<0.01$, $^{\#\#\#}p<0.001$.

cell death (Fig. 1F), revealing an increase in DNA fragmentation, particularly in the 50 MP-treated group, as confirmed by DAB staining. Western blotting results corroborated these findings: in the 50 MP-treated organoids, the expression of BAX, cytochrome C, and cleaved caspase-3 increased, indicating the activation of apoptotic pathways driven by elevated inflammatory factors (Fig. 1G). In contrast, the 100 MP-treated group showed increased BCL-2 expression, which may suppress BAX expression (Fig. 1G). To assess the harmful potential of infiltrated MP on the cerebral organoids, we conducted total RNA sequencing analysis. The analysis revealed up- and down-regulation of approximately 1300 genes or more compared to the control group in both the 50 and 100 MP treatment groups (Supplementary Fig. 1A). Among these genes, 1389 were upregulated, and 1306 were downregulated in the 50 MP treatment group (Supplementary Fig. 1B), while in the 100 MP group, 1284 genes were upregulated, and 1311 were downregulated (Supplementary Fig. 1C).

Effect of MP on neurotoxicity-related RNA expression in cerebral organoids

We performed PCR analysis to investigate neurotoxicity-related gene expression. A heatmap of the brain organoid array treated with MP is shown in Fig. 2A. 16 neurotoxicity-related genes were found to be overexpressed in the 50 MP group compared to the control (Fig. 2A, Supplementary Table 1). No genes were downregulated following MP treatment. However, we observed changes in the expression of apoptosis-related genes (BIK and FASLG) and significant alterations in metabolism-related genes (DDIT3, POU1F1, TP53, and IL-10) (Fig. 2B). Regarding neurotoxicity, significant alterations were noted in genes related to neuron development (EREG, DRP2, MMP9), ion transport (CLCNKA), nitric oxide response (NOSTRIN, ARG1), and neurotoxic signal transduction (CD8B, CIDEA, CIDEB, CDKN1A). In the 100 MP treatment group (Fig. 2C), PCR array analysis revealed an increase in the apoptosis-related gene BIK, as well as changes in EREG (neuron development), NOSTRIN (nitric oxide response), and CD8B (neurotoxic signal transduction). However, these changes were less pronounced compared to the 50 MP group. No significant changes in metabolism or ion transporter gene expression were observed in the 100 MP treatment group.

Effect of MP on neurochemical expression levels in cerebral organoids

We conducted mass spectrometry-based neurochemical analysis to assess neurotransmitter release in cerebral organoids. The neurochemical data are summarized in Supplementary Fig. 2. Acetylcholine (ACH) is a neurotransmitter that plays a critical role in cognitive functions such as memory, learning, attention, and arousal (Huang *et al*., 2022). The results showed a significant decrease in cholinergic-related ACH, suggesting potential disruptions in brain nerve conduction, slower information transmission, and a possible contribution to the progression of dementia, including Alzheimer's disease (Fig. 3A). Additionally, there was a significant increase in levels of L-kynurenine (KYN) and 3-hydroxy-DL-kynurenine (3-HK), which in turn led to an increase in tryptophan (TRP) metabolite-related effects induced by MP exposure (Fig. 3B, 3C).

Effect of MP in an *in vivo* mouse model

We conducted *in vivo* experiments to assess the effects of MP in a mouse model. Plasma MP concentrations were measured using fluorescence tagged to MP and compared to a standard curve (Fig. 4A). Brain tissue homogenates were analyzed for fluorescence expression, normalized to protein levels (Fig. 4B), revealing a significant increase in fluorescence in the brain. To assess liver toxicity, changes in AST and ALT levels were measured in the blood. Histological analysis of

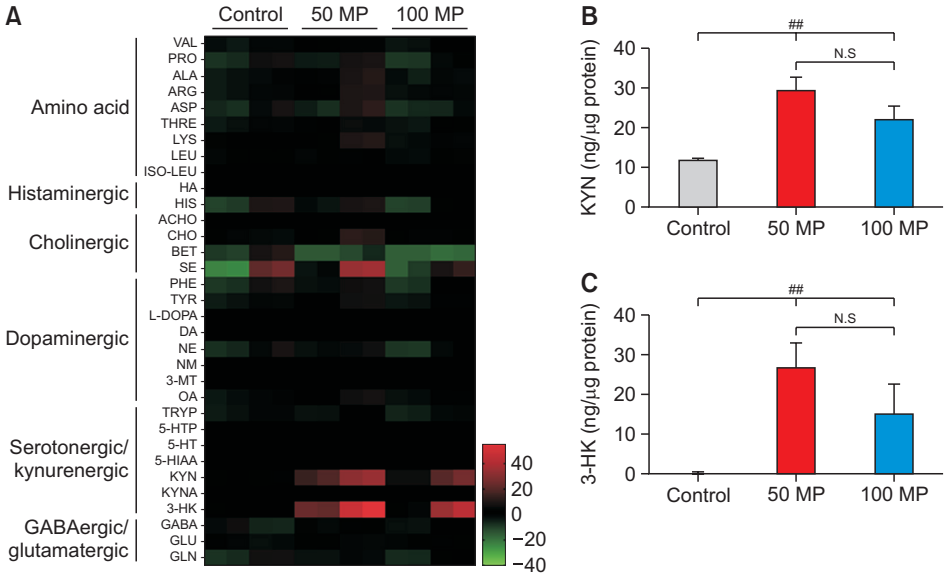

Fig. 3. Changes in neurochemical expression levels in cerebral organoids in the presence of MPs. (A) Heatmap. (B) Kynurenine expression. (C) 3-HK expression in the presence of MPs. Error bars represent the standard error of the mean from three independent experiments. $^{\#\#}p<0.01$.

liver sections stained with H&E confirmed MP infiltration into the liver parenchyma (Fig. 4C). Dot blot analysis of mouse brain homogenates revealed increased levels of 16 inflammation-related factors in the 50 MP treatment group (Supplementary Fig. 3A). Gene expression analysis also indicated an increase in inflammation-related genes in both the 50 and 100 MP-treated mice compared to the control (Supplementary Fig. 3B). Notably, proinflammatory cytokines, such as Cluster of Differentiation 93 (CD93), Cluster of Differentiation 14 (CD14), Cluster of Differentiation 40 (CD40), endostatin, fetuin A, insulin-like growth factor binding protein 2 (IGFBP-2), insulin-like growth factor binding protein 5 (IGFBP-5), osteopontin (OPN), and retinol binding protein 4 (RBP4), were all increased more than 2-fold in the 50 MP-treated group compared to the control (Supplementary Fig. 3). A TUNEL assay indicated a significant increase in DNA fragmentation in the brains of mice treated with 50 MP compared to the control (Fig. 4D, with whole brain images in Supplementary Fig. 4). These findings suggest MP-induced toxicity. We hypothesized that if cell inflammation and death occurred, microglia—the immune cells of the brain—would increase in number. This was confirmed by staining for Iba-1 and CD68, which showed increased expression of these markers in the 50 MP-treated group (Fig. 4E, with whole brain images in Supplementary Fig. 5).

Effect of MP on neurotoxicity-related RNA expression in mouse brain

We examined the effects of MP exposure on neurotoxicity-related RNA levels in the mouse brain (Fig. 5A). The data indicate significant increases in RNA expression related to apoptosis (FAS, CASP7, etc., Fig. 5B), metabolism (IL-10, TRP53, etc., Fig. 5C), and neuronal development (MMP9, HEPH, Fig. 5D) upon administration of 50 MP. Genes involved in ion transport (CLCNKA, TRPM1, etc., Fig. 5E), nitric oxide response (Fig. 5F), and signal transduction (Fig. 5G) were also significantly upregulated in the 50 MP-treated mice compared to controls.

Effect of MP on neurochemical expression levels in mouse brain

Neurochemical analysis of the mouse brain following 50 MP administration revealed changes in neurotransmitter release. The heatmap data show increased levels of KYN, 3-HK, and GLN, while NM and ACH release levels decreased (Fig. 6A). Similar to the cerebral organoids, KYN (Fig. 6B) and 3-HK (Fig. 6C) release levels were significantly elevated in the mouse brain after 50 MP administration.

DISCUSSION

In a previous study (Park *et al*., 2023), we uncovered the potential for MP to induce inflammatory colitis through exposure using colon organoids and animal models. In those experiments, MP smaller than 100 nm were found to penetrate colon organoids and induce cytotoxicity. Additionally, other studies suggest that MP of nanometer size may cross the blood-brain barrier (BBB) (Kopatz *et al*., 2023). To assess the potential toxicity of MP in the brain, we initially examined their infiltration into cerebral organoids, considering the size of the MP. As anticipated, we confirmed that smaller MP (50 nm) penetrated deeper into the cerebral organoids.

In our viability assessment, aimed at evaluating the toxicity of MP deposited on cerebral organoids, we observed a concentration-dependent decrease in viability. These results align with previous studies and support the notion that MP can reduce both cell and organoid viability. Moreover, RNA expression profile analysis revealed significant alterations in inflammatory factors, which were paralleled by a corresponding increase in protein expression. Genes associated with apoptosis and cytotoxic T-cell activity (e.g., Fas ligand, FASLG), programmed cell death (Death-Associated Protein

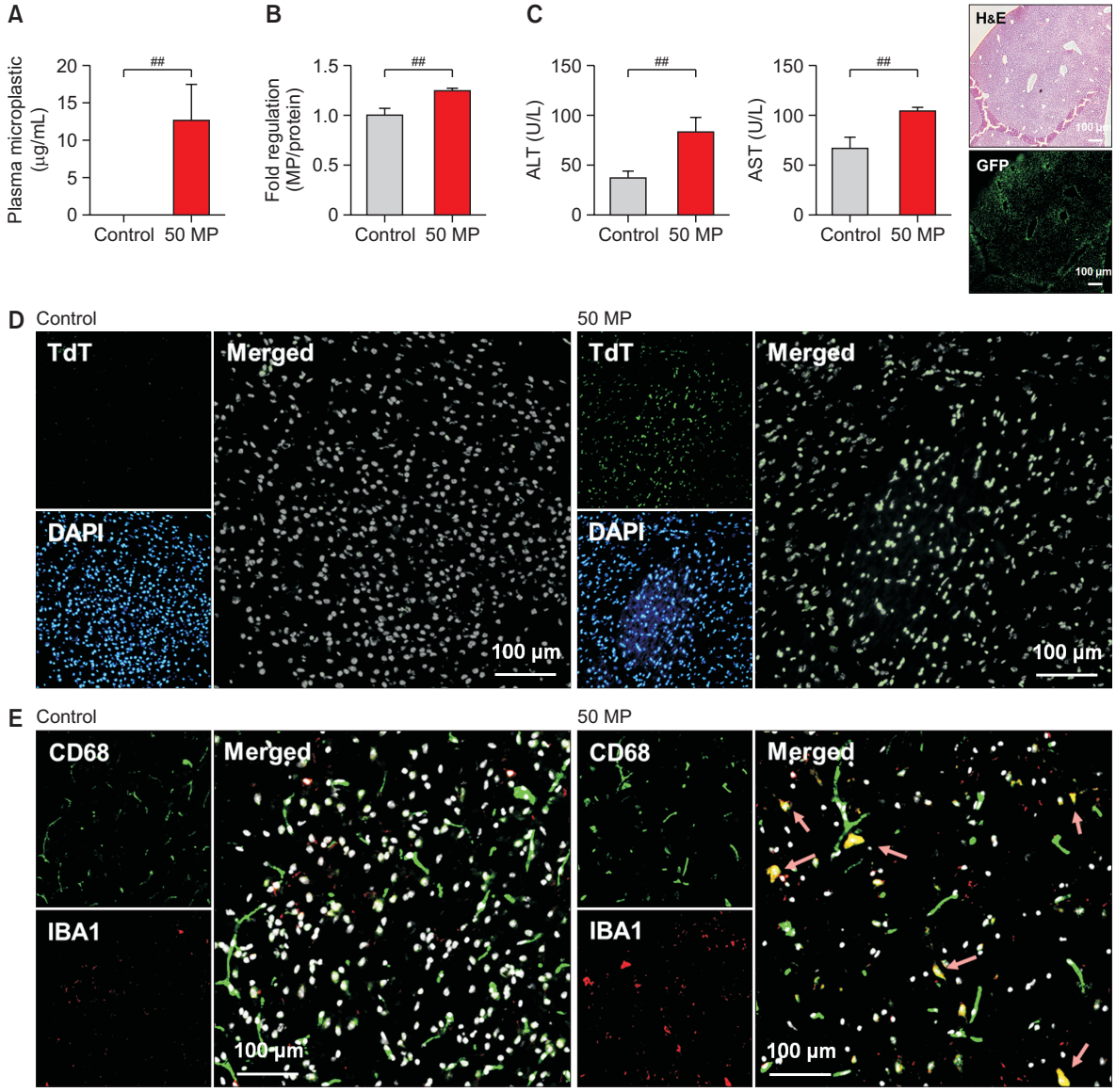

Fig. 4. Accumulation and penetration of MPs in a mouse model. (A) Detection of MPs. (B) Normalization of MP levels in mouse plasma based on protein concentration. (C) Changes in ALT and AST levels in the mouse brain. (D) Immunofluorescence images of TdT. (E) Immunofluorescence images of CD68 and IBA1 in the presence of 50 nm MPs in the mouse brain. Error bars represent the standard error of the mean from three independent experiments. $^{\#\#}p<0.01$.

Kinase 1, DAPK1), and potential DNA damage leading to cell cycle arrest (Cyclin-Dependent Kinase Inhibitor 1, CDKN1A) were all upregulated in the 50 MP group compared to the control. These findings are consistent with other studies suggesting that exposure to microplastics may trigger inflammatory responses in both animals and humans.

However, changes in gene expression related to inflammation alone may not fully elucidate MP-induced apoptosis in cerebral organoids. To address this, we conducted Western blotting to evaluate cell death, confirming that apoptosis was triggered by an increase in inflammatory factors. Notably, the 50 nm MP-treated cerebral organoids exhibited an increase in BAX expression, followed by an upsurge in cytochrome C expression and activation of caspase 3, indicating proper progression of the apoptosis signaling pathway. The mechanism responsible for the overexpression of BCL-2 in the 100 nm MP-treated organoids remains unclear; however, larger MP (100 nm) may suppress apoptosis due to their limited penetration into cerebral organoids.

We also evaluated the toxic effects of MP on the mouse brain. A notable increase in DNA fragmentation was observed in the hippocampus and cortex regions of the brain in 50 nm MP-treated mice, but no significant changes were observed in other blood parameters. Increased microglial expression was detected in the hypothalamus (Hy), pons and medulla (PM), hippocampus (Hi), and cerebral cortex (Cx), but not in the olfactory bulb (OB) or basal forebrain (BF). These results provide additional evidence of the potentially harmful effects of

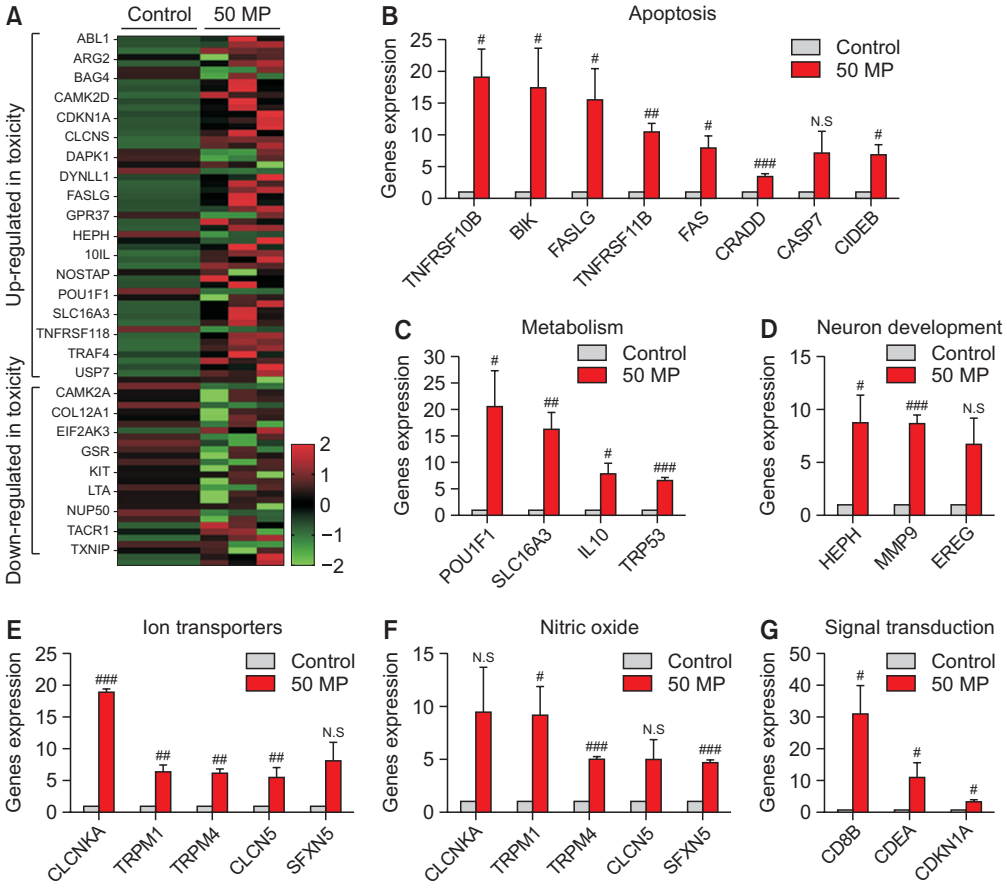

Fig. 5. Effect of MPs on neurotoxicity in the mouse brain. (A) Heatmap of changes in neurotoxicity-related gene expression levels. (B) Apoptosis-related gene expression. (C) Metabolism-related gene expression. (D) Neuronal development-related gene expression. (E) Ion transporter-related gene expression. (F) Nitric oxide-related gene expression. (G) Signal transduction-related gene expression in the presence of 50 nm MPs in the mouse brain. Error bars represent the standard error of the mean from three independent experiments. $^{\#}p<0.05$, $^{\#\#}p<0.01$, $^{\#\#\#}p<0.001$.

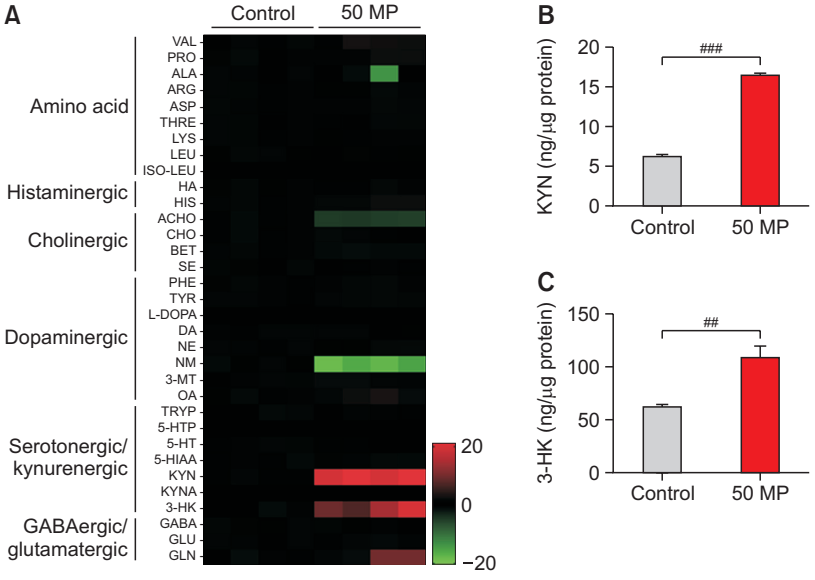

Fig. 6. Changes in neurochemical expression levels in the mouse brain in the presence of MPs. (A) Heatmap. (B) Kynurenine expression. (C) 3-HK expression in the presence of MPs. Error bars represent the standard error of the mean from three independent experiments. $^{\#\#}p<0.01$, $^{\#\#\#}p<0.001$.

MP on the mouse brain, emphasizing neurotoxicity and functional alterations in neurotransmitter systems.

Recent studies involving various mammals have highlighted the neurotoxic effects of MP (Ye *et al*., 2023). Cell-level studies have demonstrated increased uptake of MP and neurotoxic responses (Prüst *et al*., 2020). Research using zebrafish models has revealed various behavioral changes, including hyperactivity and motor dysfunction, indicating the potential for neurotoxicity following MP exposure (Liu *et al*., 2021; Aliakbarzadeh *et al*., 2023). Other studies have shown that MP induce neurotoxicity through oxidative stress, alterations in neurotransmitter levels, and inhibition of acetylcholinesterase activity after crossing the BBB (Barboza *et al*., 2018; Xiong *et al*., 2023). Our neurotransmitter metabolome analysis of cerebral organoids and mouse brains revealed an increase in the tryptophan pathway, which is involved in serotonin (5-HT) synthesis, following MP administration in both cerebral organoids and *in vivo* mouse models. In mammals, the majority of tryptophan follows the kynurenic pathway, leading to the conversion of tryptophan into bioactive compounds such as kynurenine (KYN). Exposure to MP may heighten the production of tryptophan-based bioactive substances. Given that most tryptophan enters the kynurenic pathway, even slight changes in this pathway can result in neurotoxicity within the brain (Guillemin *et al*., 2006; Ramirez Ortega *et al*., 2020). Our results indicated an increase in KYN and 3-HK following MP administration. Tryptophan metabolism is divided into two pathways: the serotonergic pathway for the synthesis of 5-HT and the kynurenic pathway for the production of kynurenine. In an inflammatory state, the kynurenic pathway becomes more activated, leading to the production of neurotoxic molecules such as 3-HK and quinolinic acid (QA) (Guidetti *et al*., 2000; Zinger *et al*., 2011; Schwarcz *et al*., 2012). The results of this study show metabolic activation of KYN to 3-HK in brain organoids and mouse brain tissues exposed to MP (Fig. 7). Our findings on kynurenine pathway activation and its role in neurotoxicity upon MP exposure may further advance our understanding of the mechanisms underlying MP-induced neurotoxicity.

While cerebral organoids provide valuable insights into MP toxicity, it is important to recognize their limitations. These models do not fully replicate the complexity of the adult human brain and may not precisely mimic the intricate interactions between different cell types and brain regions. Nevertheless, they serve as invaluable tools for initial screening, identifying potential mechanisms of MP toxicity, and guiding further investigations aimed at developing strategies to mitigate their detrimental effects on brain health, in conjunction with *in vivo* studies.

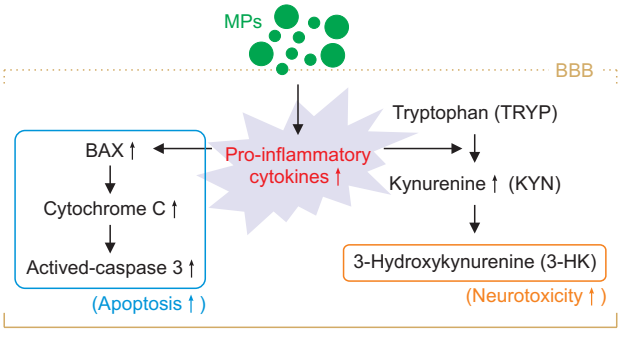

Fig. 7. Potential mechanism of microplastics (MP)-induced neurotoxicity.

Although the exact metabolic pathway is not yet fully understood, microplastics are believed to accumulate in the body and regulate the expression of metabolites closely associated with inflammation, cell death, neurotoxicity, and carcinogenicity. Our findings represent the first report demonstrating that MP can induce neurotoxicity by promoting the synthesis of the neurotoxic molecule 3-HK through the induction of a neuroinflammatory state after crossing the BBB and accumulating in the brain. This leads to an elevated biosynthesis of neurotoxic substances, such as quinolinic acid, which can impact brain development and physiological processes.

CONFLICT OF INTEREST

The authors have no potential conflicts of interest.

ACKNOWLEDGMENTS

The authors greatly acknowledge financial support from the Ministry of Science and ICT (2021R1A2C2011195), the Ministry of Trade, Industry & Energy (20009774) and the Korea Research Institute of Chemical Technology (KK2431-10) of Republic of Korea.

REFERENCES

Aliakbarzadeh, F., Rafiee, M., Khodagholi, F., Khorramizadeh, M. R, Manouchehri, H., Eslami, A., Sayehmiri, F. and Mohseni-Bandpei, A. (2023) Adverse effects of polystyrene nanoplastic and its binary mixtures with nonylphenol on zebrafish nervous system: from oxidative stress to impaired neurotransmitter system. *Environ. Pollut.* **317**, 120587.

Brémond Martin, C., Simon Chane, C., Clouchoux, C. and Histace, A. (2021) Recent trends and perspectives in cerebral organoids imaging and analysis. *Front. Neurosci.* **15**, 629067.

Barboza, L. G. A., Vieira, L. R., Branco, V., Figueiredo, N., Carvalho, F., Carvalho, C. and Guilhermino, L. (2018) Microplastics cause neurotoxicity, oxidative damage and energy-related changes and interact with the bioaccumulation of mercury in the european seabass, Dicentrarchus labrax (Linnaeus, 1758). *Aquat. Toxicol.* **195**, 49-57.

Cakir, B., Xiang, Y., Tanaka, Y., Kural, M. H., Parent, M., Kang, Y.-J., Chapeton, K., Patterson, B., Yuan, Y., He, C.-S., Raredon, M. S. B., Dengelegi, J., Kim, K.-Y., Sun, P., Zhong, M., Lee, S., Patra, P., Hyder, F., Niklason, L. E., Lee, S.-H., Yoon, Y.-S. and Park, I.-H. (2019) Engineering of human brain organoids with a functional vascular-like system. *Nat. Methods* **16**, 1169-1175.

Cocci, P., Gabrielli. S., Pastore, G., Minicucci, M., Mosconi, G. and Palermo, F. A. (2022) Microplastics accumulation in gastrointestinal tracts of Mullus barbatus and Merluccius merluccius is associated with increased cytokine production and signaling. *Chemosphere* **307**, 135813.

Fan, P., Wang, Y., Xu, M., Han, X., Liu, Y. (2022) The application of brain organoids in assessing neural toxicity. *Front. Mol. Neurosci.* **15**, 799397.

Fu, Q., Tan, X., Ye, S., Ma, L., Gu, Y., Zhang, P., Chen, Q., Yang, Y. and Tang, Y. (2021) Mechanism analysis of heavy metal lead captured by natural-aged microplastics. *Chemosphere* **270**, 128624.

Guidetti, P., Reddy, P. H., Tagle, D. A. and Schwarcz, R. (2000) Early kynurenergic impairment in Huntington's disease and in a transgenic animal model. *Neurosci. Lett.* **283**, 233-235.

Guillemin, G. J., Meininger, V. and Brew, B. J. (2006) Implications for the kynurenine pathway and quinolinic acid in amyotrophic lateral sclerosis. *Neurodegener. Dis.* **2**, 166-176.

Hale, R. C., Seeley, M. E., La Guardia, M. J., Mai, L. and Zeng, E. Y. (2020) A global perspective on microplastics. *J. Geophysical. Res. Oceans* **125**, e2018JC014719.

Han, J. Y., Lee, E.-H., Kim, S.-M. and Park, C.-H. (2023) Efficient generation of dopaminergic neurons from mouse ventral midbrain astrocytes. *Biomol. Ther. (Seoul)* **31**, 264-275.

Hua, T., Kiran, S., Li, Y. and Sang, Q.-X. A. (2022) Microplastics exposure affects neural development of human pluripotent stem cell-derived cortical spheroids. *J. Hazard. Mater.* **435**, 128884.

Huang, Q., Liao, C., Ge, F., Ao, J. and Liu, T. (2022) Acetylcholine bidirectionally regulates learning and memory. *J. Neurorestoratology* **10**, 100002.

Jeong, B., Baek, J. Y., Koo, J., Park, S., Ryu, Y.-K., Kim, K.-S., Zhang, S., Chung, C., Dogan, R., Choi, H.-S., Um, D., Kim, T.-K., Lee, W. S., Jeong, J., Shin, W.-H., Lee, J.-R., Kim, N.-S. and Lee, D. Y. (2022) Maternal exposure to polystyrene nanoplastics causes brain abnormalities in progeny. *J. Hazard. Mater.* **426**, 127815.

Jeong, J.-H., Kim, D.-J., Hong, S.-J., Ahn, J.-H., Lee, D.-J., Jang, A.-R., Kim, S., Cho, H.-J., Lee, J.-Y., Park, J.-H., Kim, Y.-M. and Ko, H.-J. (2024) Investigating the immune-stimulating potential of β-glucan from aureobasidium pullulans in cancer immunotherapy. *Biomol. Ther. (Seoul)* **32**, 556-567.

Jin, H., Yang, C., Jiang, C., Li, L., Pan, M., Li, D., Han, X. and Ding, J. (2022) Evaluation of neurotoxicity in BALB/c mice following chronic exposure to polystyrene microplastics. *Environ. Health Perspect.* **130**, 107002.

Kang, G. J., Park, J. H., Kim, H. J., Kim, E. J., Kim, B., Byun, H. J., Yu, L., Nguyen, T. M., Nguyen, T. H., Kim, K. S., Huy, H. P., Rahman, M., Kim, Y. H., Jang, J. Y., Park, M. K., Lee, H., Choi, C. I., Lee, K., Han, H. K., Cho, J., Rho, S. B. and Lee, C. H. (2022) PRR16/Largen induces epithelial-mesenchymal transition through the interaction with ABI2 leading to the activation of ABL1 kinase. *Biomol. Ther. (Seoul)* **30**, 340-347.

Kaushik, A., Singh, A., Kumar Gupta, V. and Mishra, Y. K. (2024) Nano/micro-plastic, an invisible threat getting into the brain. *Chemosphere* **361**, 142380.

Kelley, K. W. and Pașca, S. P. (2022) Human brain organogenesis: Toward a cellular understanding of development and disease. *Cell* **185**, 42-61.

Kim, S. S., Lee, H. Y., Song, J. S., Bae, M. A. and Ahn, S. (2021) UPLC-MS/MS-based profiling of 31 neurochemicals in the mouse brain after treatment with the antidepressant nefazodone. *Microchem. J.* **169**, 106580.

Kopatz, V., Wen, K., Kovács, T., Keimowitz, A. S., Pichler, V., Widder, J., Vethaak, A. D., Hollóczki, O. and Kenner, L. (2023) Micro- and nanoplastics breach the blood-brain barrier (BBB): biomolecular Corona's role revealed. *Nanomaterials* **13**, 1404.

Lancaster, M. A., Renner, M., Martin, C.-A., Wenzel, D., Bicknell, L. S., Hurles, M. E., Homfray, T., Penninger, J. M., Jackson, A. P. and Knoblich, J. A. (2013) Cerebral organoids model human brain development and microcephaly. *Nature* **501**, 373-379.

Lee, C.-W., Hsu, L.-F., Wu, I.-L., Wang, Y.-L., Chen, W.-C., Liu, Y.-J., Yang, L.-T., Tan, C.-L., Luo, Y.-H., Wang, C.-C., Chiu, H.-W., Yang, T. C. K., Lin, Y.-Y., Chang, H.-A., Chiang, Y.-C., Chen, C.-H., Lee, M.-H., Peng, K.-T. and Huang, C. C. Y. (2022) Exposure to polystyrene microplastics impairs hippocampus-dependent learning and memory in mice. *J. Hazard. Mater.* **430**, 128431.

Li, M., Gong, J., Gao, L., Zou, T., Kang, J. and Xu, H. (2022) Advanced human developmental toxicity and teratogenicity assessment using human organoid models. *Ecotoxicol. Environ. Saf.* **235**, 113429.

Liu, Y., Wang, Y., Ling, X., Yan, Z., Wu, D., Liu, J. and Lu, G. (2021) Effects of nanoplastics and butyl methoxydibenzoylmethane on early zebrafish embryos identified by single-cell RNA sequencing. *Environ. Sci. Technol.* **55**, 1885-1896.

Lu, X., Hu, H., Li, J., Li, J., Wang, L., Liu, L. and Tang, Y. (2023) Microplastics existence affected heavy metal affinity to ferrihydrite as a representative sediment mineral. *Sci. Total Environ.* **859**, 160227.

Mohamed Nor, N. H., Kooi, M., Diepens, N. J. and Koelmans, A. A. (2021) Lifetime accumulation of microplastic in children and adults. *Environ. Sci. Technol.* **55**, 5084-5096.

Park, I. G., Jin, S. H., An, S., Ki, M. W., Park, W. S., Kim, H.-J., Na, Y. and Noh, M. (2024) Carnosine and retinol synergistically inhibit UVB-induced PGE2 synthesis in human keratinocytes through the up-regulation of hyaluronan synthase 2. *Biomol. Ther. (Seoul)* **31**, 635-639.

Park, S. B., Jung, W. H., Choi, K. J., Koh, B. and Kim, K. Y. (2023) a comparative systematic analysis of the influence of microplastics on colon cells, mouse and colon organoids. *Tissue Eng. Regen. Med.* **20**, 49-58.

Parmentier, T., LaMarre, J. and Lalonde, J. (2023) Evaluation of neurotoxicity with human pluripotent stem cell-derived cerebral organoids. *Curr. Protoc.* **3**, e744.

Pitt, J. A., Kozal, J. S., Jayasundara, N., Massarsky, A., Trevisan, R., Geitner, N., Wiesner, M., Levin, E. D. and Di Giulio, R. T. (2018) Uptake, tissue distribution, and toxicity of polystyrene nanoparticles in developing zebrafish. *Aquat. Toxicol.* **194**, 185-194.

Pollen, A. A., Bhaduri, A., Andrews, M. G., Nowakowski, T. J., Meyerson, O. S., Mostajo-Radji, M. A., Di Lullo, E., Alvarado, B., Bedolli, M., Dougherty, M. L., Fiddes, I. T., Kronenberg, Z. N., Shuga, J., Leyrat, A. A., West, J. A., Bershteyn, M., Lowe, C. B., Pavlovic, B. J., Salama, S. R., Haussler, D., Eichler, E. E. and Kriegstein, A. R. (2019) Establishing cerebral organoids as models of human-specific brain evolution. *Cell* **176**, 743-756.e17.

Prüst, M., Meijer, J. and Westerink, R. H. S. (2020) The plastic brain: neurotoxicity of micro- and nanoplastics. *Part. Fibre Toxicol.* **17**, 24.

Qian, X., Song, H. and Ming, G.-L. (2019) Brain organoids: advances, applications and challenges. *Development* **146**, dev166074.

Ramirez Ortega, D., Ovalle Rodríguez, P., Pineda, B., González Esquivel, D. F., Ramos Chávez, L. A., Vázquez Cervantes, G. I., RoldánRoldán, G., Pérez de la Cruz, G., Díaz Ruiz, A., Méndez Armenta, M., Marcial Quino, J., Gómez Manzo, S., Ríos, C. and Pérez de la Cruz, V. (2020) Kynurenine pathway as a new target of cognitive impairment induced by lead toxicity during the lactation. *Sci. Rep.* **10**, 3184.

Rivers-Auty, J., Bond, A. L., Grant, M. L. and Lavers, J. L. (2023) The one-two punch of plastic exposure: Macro- and micro-plastics induce multi-organ damage in seabirds. *J. Hazard. Mater.* **442**, 130117.

Samy, J. V. R. A., Kumar, N., Singaravel, S., Krishnamoorthy, R., Alshuniaber, M. A., Gatasheh, M. K., Venkatesan, A., Natesan, V. and Kim, S.-J. (2023) Effect of prunetin on streptozotocin-induced diabetic nephropathy in rats - a biochemical and molecular approach. *Biomol. Ther. (Seoul)* **31**, 619-628.

Schwarcz, R., Bruno, J. P., Muchowski, P. J. and Wu, H.-Q. (2012) Kynurenines in the mammalian brain: when physiology meets pathology. *Nat. Rev. Neurosci.* **13**, 465-477.

Teng, M., Zhao, X., Wang, C., Wang, C., White, J. C., Zhao, W., Zhou, L., Duan, M. and Wu, F. (2022) Polystyrene nanoplastics toxicity to zebrafish: dysregulation of the brain-intestine-microbiota axis. *ACS Nano* **16**, 8190-8204.

Velasco, S., Kedaigle, A. J., Simmons, S. K., Nash, A., Rocha, M., Quadrato, G., Paulsen, B., Nguyen, L., Adiconis, X., Regev, A., Levin, J. Z. and Arlotta, P. (2019) Individual brain organoids reproducibly form cell diversity of the human cerebral cortex. *Nature* **570**, 523-527.

Vethaak, A. D. and Legler, J. (2021) Microplastics and human health. *Science* **371**, 672-674.

Xiang, Y., Tanaka, Y., Patterson, B., Kang, Y.-J., Govindaiah, G., Roselaar, N., Cakir, B., Kim, K.-Y., Lombroso, A. P., Hwang, S.-M., Zhong, M., Stanley, E. G., Elefanty, A. G., Naegele, J. R., Lee, S.-H., Weissman, S. M. and Park, I.-H. (2017) Fusion of regionally specified hPSC-derived organoids models human brain development and interneuron migration. *Cell Stem Cell* **21**, 383-398.

Xiong, F., Liu, J., Xu, K., Huang, J., Wang, D., Li, F., Wang, S., Zhang, J., Pu, Y. and Sun, R. (2023) Microplastics induce neurotoxicity in aquatic animals at environmentally realistic concentrations: a meta-analysis. *Environ. Pollut.* **318**, 120939.

Xu, J.-L., Lin, X., Wang, J. J. and Gowen, A. A. (2022) A review of potential human health impacts of micro- and nanoplastics exposure. *Sci. Total Environ.* **851**, 158111.

Ye, Z., Mai, T., Cheng, Y., Zhang, X., Liu, Z., Zhang, Z. and Li, Y. (2023) Neurotoxicity of microplastics: a CiteSpace-based review and emerging trends study. *Environ. Monit. Assess.* **195**, 960.

Yuan, Z., Nag, R. and Cummins, E. (2022) Human health concerns regarding microplastics in the aquatic environment - from marine to food systems. *Sci. Total Environ.* **823**, 153730.

Zhou, Y., Peng, Z., Seven, E. S. and Leblanc, R. M. (2018) Crossing the blood-brain barrier with nanoparticles. *J. Control. Release* **270**, 290-303.

Zinger, A., Barcia, C., Herrero, M. T. and Guillemin, G. J. (2011) The involvement of neuroinflammation and kynurenine pathway in Parkinson's disease. *Parkinsons Dis.* **2011**, 716859.